BJR

https://doi.org/10.1259/bjr.20200250

Received: 16 March 2020 | Revised: 28 May 2020 | Accepted: 01 June 2020

Cite this article as:
Gennaro N, Marrari A, Renne SL, Cananzi FCM, Quagliuolo VL, Di Brina L, et al. Multimodality imaging of adult rhabdomyosarcoma: the added value of hybrid imaging. *Br J Radiol* 2020; **93**: 20200250.

PICTORIAL REVIEW

Multimodality imaging of adult rhabdomyosarcoma: the added value of hybrid imaging

[1,2]NICOLÒ GENNARO, MD, [1,3]ANDREA MARRARI, MD, [1,4]SALVATORE LORENZO RENNE, MD, [1,5]FERDINANDO CARLO MARIA CANANZI, MD, [5]VITTORIO LORENZO QUAGLIUOLO, MD, [6]LUCIA DI BRINA, MD, [1,6,7]MARTA SCORSETTI, MD, [8]GIOVANNA PEPE, MD, [1,7,8]ARTURO CHITI, MD, [1,3,7]ARMANDO SANTORO, MD, [2]LUCA BALZARINI, MD, [7,9,10,11]LETTERIO SALVATORE POLITI, MD and [3]ALEXIA FRANCESCA BERTUZZI, MD

[1]Dept. of Biomedical Sciences, Humanitas University, Pieve Emanuele, Italy
[2]Dept. of Radiology, Humanitas Clinical and Research Center - IRCCS, Rozzano, Italy
[3]Medical Oncology and Hematology Unit, Humanitas Clinical and Research Center, IRCCS, Rozzano, Italy
[4]Dept. of Pathology, Humanitas Clinical and Research Hospital - IRCCS, Rozzano, Italy
[5]Sarcoma, Melanoma and Rare Tumors Surgery Unit, Humanitas Clinical and Research Center - IRCCS, Rozzano, Italy
[6]Dept. of Radiation Oncology, Humanitas Clinical and Research Center - IRCCS, Rozzano, Italy
[7]Dept. of Biomedical Sciences, Humanitas University, Pieve Emanuele, Italy
[8]Dept. of Nuclear Medicine, Humanitas Clinical and Research Center - IRCCS, Rozzano, Italy
[9]Neuroradiology Unit, Humanitas Clinical and Research Center - IRCCS, Rozzano, Italy
[10]Dept. of Radiology and Hematology & Oncology Division, Boston Children's Hospital, Boston, USA
[11]Dept. of Radiology and Advanced MRI Center, University of Massachusetts Medical School and Medical Center, Worcester, USA

Address correspondence to: Nicolò Gennaro
E-mail: *nicolo.gennaro@st.hunimed.eu*

ABSTRACT

Rhabdomyosarcoma (RMS) represents more than 50% of paediatric soft tissue tumours. Conversely, it is extremely rare among adults, where it shows peculiar biological and clinical features that are still poorly investigated. RMS patients should be referred to a Sarcoma Centre, where the contribution of experienced radiologists plays a relevant role in the diagnostic assessment of the disease, including precise localisation, staging, image-guided biopsy, response evaluation after treatment and follow-up. Besides CT and MRI, hybrid imaging including positron emission tomography (PET)/CT and PET/MRI are giving an increasing contribution to provide functional insights about tumour biology and to improve the diagnostic accuracy of the imaging work-up. This review paper provides a revision of the pathology, clinical and radiological features of adult RMS, with a particular focus on the growing role of hybrid PET-based imaging.

INTRODUCTION

Rhabdomyosarcomas (RMS) include a heterogeneous group of rare malignant mesenchymal cancers resembling skeletal muscle differentiation.[1] They represent >50% of soft tissue tumours in paediatric age (<16 years) with an incidence of 4 cases per million/year. Conversely, the same tumours are unusual in the non-paediatric population, accounting for 11% of cancers in adolescents and only 1–2% in the adult population.[2]

Imaging plays a major role in the management of RMS through a comprehensive diagnostic assessment that includes extent of the primary tumour, the nodal status, image-guided biopsy, evaluation of treatment response and follow-up. Similarly to other oncohaematological diseases, hybrid imaging including PET/CT and PET/MR improves such evaluation through metabolic insights of tumour biology. The aim of this paper is to provide a comprehensive review of the imaging of adult RMS correlated with the clinicopathological characteristics, focusing on the growing role of hybrid PET-based modalities.

PATHOLOGY

RMS are the malignant tumours with features of skeletal-muscle differentiation, according to morphology and immunohistochemistry.[3] The revised 2013 World Health Organisation (WHO) classification, which takes into account new cytogenetic and molecular criteria in addition of morphology, identifies four histological variants—alveolar, embryonal, spindle cell/sclerosing and pleomorphic RMS (Figure 1). Alveolar (aRMS) and embryonal (eRMS) RMS, typical of the paediatric population, belong to the family of small round cell sarcomas and are therefore labelled as high-grade tumours.[4] Conversely, spindle cell/sclerosing

Figure 1. General overview of soft tissue tumours listed in the WHO classification released in 2013.

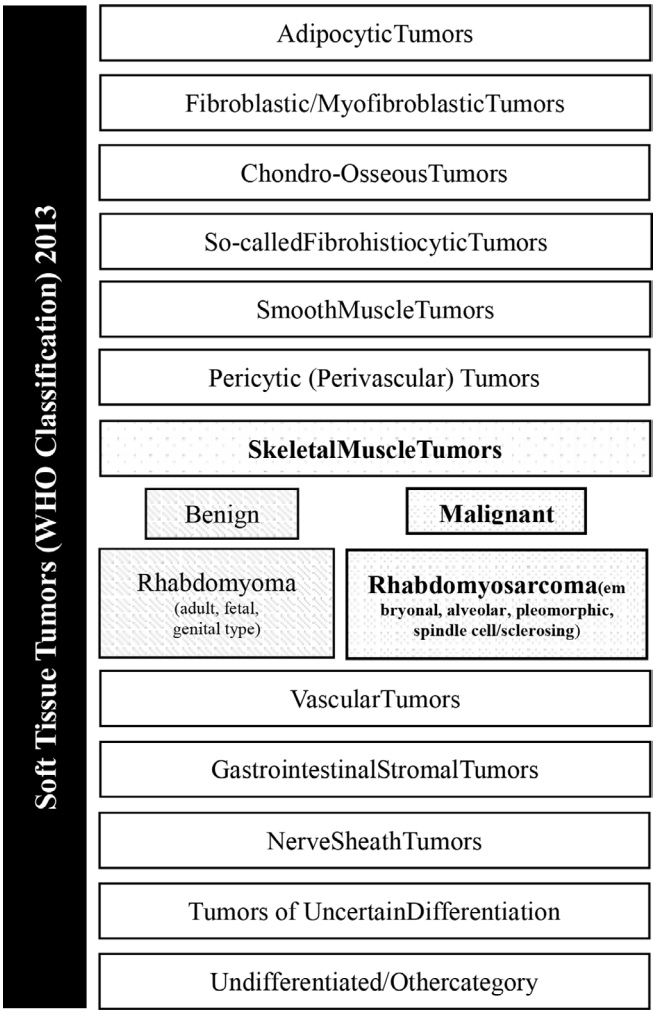

and pleomorphic RMS are graded according to the Fédération Nationale des Centres de Lutte le Cancer (FNCLCC) grading system, which accounts for tumour differentiation, mitosis and necrosis.[5] aRMS and eRMS display a more easily recognisable rhabdomyoblastic differentiation than sclerosing/spindle cell and pleomorphic subtypes, defined by immunohistochemical positivity for desmin, myogenin or MYOD1. eRMS is characterised by the admixture of cellular and myxoid areas, wherein cells present eccentric vesicular nuclei and eosinophilic cytoplasm (Figure 2a–b). aRMS is composed of primitive cells with monomorphous round nuclei and owes its name to the collagenous septa that separate tumour cells into discrete nests, resembling lung alveoli (Figure 2c–d). Gene translocations involving Pax3 or seven and FOX01 are identified in most alveolar RMS, which are called "fusion-positive". Spindle cell/sclerosing RMS represents a spectrum of RMS variants that share spindle cell morphology, including emerging entities with unique molecular and genetic features, such as VGLL2/NCOA2 and TFCP2 rearrangement or MYOD1 mutation (Figure 2e–f).[6] Pleomorphic RMS is a less-differentiated histological variant composed of sheets of large, atypical, and multinucleated polygonal eosinophilic cells or undifferentiated round-to-spindle cells (Figure 2g–h).

Figure 2. eRMS (a) At high power view (400x), cross-striation in cells can be noticed (arrow), as well as cytoplasmic eosinophilia in rhabdomyoblasts (arrowheads). Cells are spindle and mild heterogeneity in shape and size is appreciated. Immunohistochemistry positivity for Myogenin (b) and Desmin (right upper panel); aRMS. (c) At high power examination (400x) the characteristic "alveolar" appearance is depicted: tumour cells are separated by fibrovascular septa, at the periphery of which, the cells line the septa, whilst centrally, far from the septa, cells are less cohesive; cells are round shaped, with monomorphous appearance and few eccentric nuclei. (d) Cells are strongly positive for myogenin and desmin (right upper panel); Spindle cell/sclerosing RMS. (e) At higher power view (400x) hyperchromatic and elongated nuclei can be observed. Spindle cell proliferation is variably intermixed with dense sclerotic stroma and positivity for both myogenin (f) and desmin (right upper panel); Pleomorphic RMS. (g) At higher magnification (400x), pleomorphic, spindle cells and several mitoses can be seen. Nuclei are hyperchromatic and nucleoli are variably present. (h) Myogenin positivity, even focal, is diagnostic whilst positivity of desmin (right upper panel) can be a common feature. RMS, rhabdomyosarcomas.

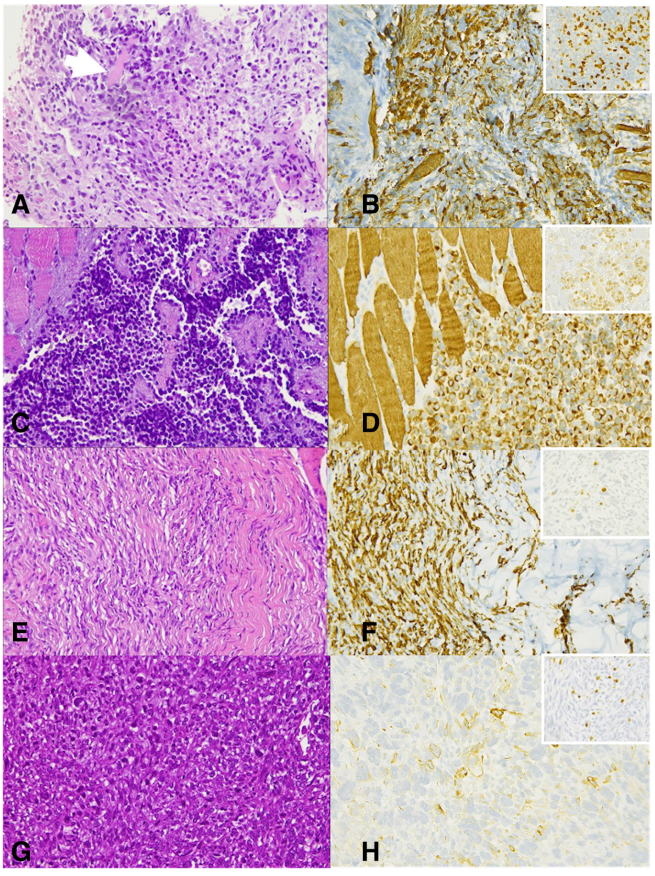

Clinical features of adult RMS

The prevalent histology in adults is the pleomorphic subtype, which is extremely rare in the paediatric population. Pleomorphic subtype accounts for more than 50% of adult RMS and increases in incidence with age. Although RMS can arise at any anatomical site, adult RMS are typically localised in the extremities (40%) (Figure 3), head and neck (30%) (Figure 4) and

Figure 3. Non-enhancing areas representing necrotic tissue (arrow) on post-contrast T_1 W image in (a) post-contrast axial T_1W image acquired at the level of the left thigh in a 39 year-old male diagnosed with pleomorphic RMS; (b) sagittal post-contrast T_1 weighted image of the right thigh of a 49-year-old male diagnosed with spindle cell/sclerosing RMS. RMS, rhabdomyosarcomas; T_1W, T_1 weighted.

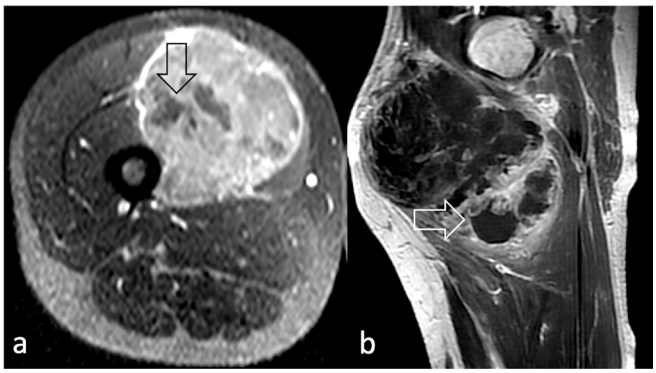

genitourinary tract (20%; Figure 5)[2]. Table 1 summarises the relevant features of each RMS subtype.

RMS usually presents with an asymptomatic mass or with signs and symptoms related to the mass effect upon adjacent structures. Compared to paediatric eARMS and aRMS, clinical presentation is more aggressive with more than 30% patients presenting regional lymph node involvement and 20% patients diagnosed with distant metastasis (Figure 6).[7,8] Also, specific gene expression is peculiar in the adult population with respect to the younger, suggesting adult RMS to be a separate entity in the RMS landscape.[9] Unlike paediatric RMS, adult RMS is seldom, if ever, part of syndromic or familiar conditions such as hereditary retinoblastoma, neurofibromatosis Type 1, Li–Fraumeni and Costello syndromes.[3] In terms of clinical outcome, the 5-year survival rate in adults is considerably poor compared to children (27% *vs* 70%), even if considering localised disease only (47% *vs* 81%).[10] The reasons for such worse outcomes remain

Figure 4. 19-year-old patient diagnosed with recurrent pleomorphic RMS. ^{11}C-Methionine PET fused with T_2 weighted MR images shows (a) in the sagittal and (b) coronal view of the lesion extending through the inferior temporal gyrus, middle cranial fossa, sellar region, masticatory space and pterygopalatine fossa (arrow). A central necrotic area is visible (asterisk). PET, positron emision tomography.

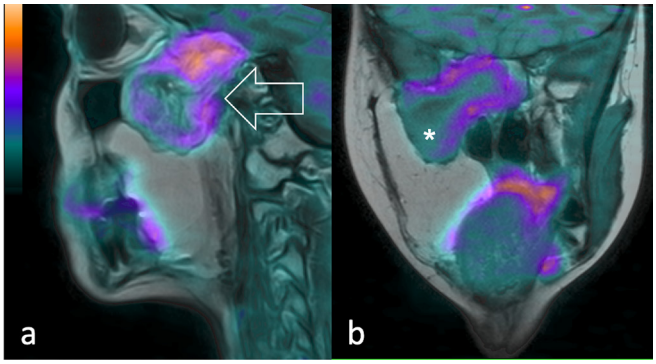

Figure 5. Same 19-year-old patient of Figure 2a–b, diagnosed with eRMS. MRI shows in (a) sagittal T_2 weighted image a voluminous, heterogeneous mass in the prostatic lodge (arrow) with (b) increased peripheral vascularisation seen in axial fat suppressed post-contrast T_1 weighted image. The patient presented with (c) ^{18}F-FDG PET/CT showed an isolated radiopharmaceutical uptake consistent with lymphadenopathy (arrow) and (d) marked signal restriction on axial DWI scan (e) ^{18}F-FDG PET/T_2W-MRI shows intense uptake at the level of the mass and multiple lung metastases in maximum intensity projection coronal plane (arrow). ^{18}F-FDG, ^{18}F-fludeoxyglucose; DWI, diffusion-weighted imaging; PET, positron emision tomography; RMS, rhabdomyosarcomas; T_2W, T_2 weighted.

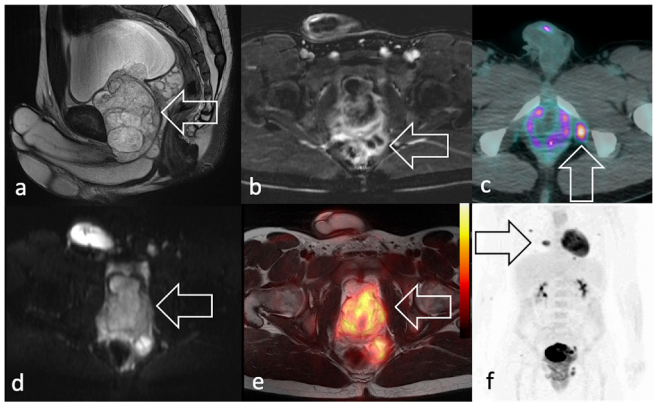

largely unknown. The intrinsic differences in tumour biology, the rarity of RMS in adult oncology, and the inability to use intensive and prolonged chemotherapy regimens as for paediatric patients have been appointed to contribute to such unsatisfactory outcomes.[10,11]

Imaging of RMS

Imaging provides comprehensive diagnostic assessment of RMS mainly through contrast-enhanced MRI and CT for local and distant staging, respectively.

However, ultrasound can be used to guide core-needle biopsy of superficial lesions (Figure 7) and may identify superficial or bulky deep-seated lymphadenopathy (Figure 8). Notably, ultrasound may provide better disease assessment in rare presentations, like thyroid RMS (Figure 9).

MRI is the imaging modality of choice for local staging of RMS due to its excellent contrast resolution for soft tissues (Figure 10). RMS appears iso- to slightly hypointense to skeletal muscle on T_1 weighted sequences, due to the hyaline collagenous stroma and slightly-to-markedly hyperintense on T_2/STIR-weighted sequences, depending on the amount of necrohaemorrhagic content. Following intravenous gadolinium contrast administration, RMS shows moderate-to-avid heterogeneous enhancement due to internal necrotic components. Necrosis is usually visualised as hypodense and hyperintense areas on CT and fluid sensitive MRI sequences, respectively (Figure 11). MRI also estimates tissue cellularity through the apparent diffusion coefficient (ADC), obtained with diffusion-weighted imaging (DWI). Such assessment can be valuable to confirm necrosis (usually

Table 1. Clinical and pathology features of each RMS subtype

Feature	Embryonal	Alveolar	Spindle cell/sclerosing	Pleomorphic
Frequent localisation	Mucosae, Urogenital, Head, Neck	Head and neck, Extremities	Head and neck	Ubiquitous
Prevalence	10–20%	20–30%	5–10%	50–60%
Prognosis	Poor	Poor	Variable	Poor
Histo-morphology	Round and spindled proliferation within a myxoidstroma	Round cells with fibrous septa	Homogeneous proliferation of spindle-like cells (spindled and sclerosing/epithelioid)	Heterogeneous cells in shape and size (pleomorphism)
Immunohistochemistry	Heterogeneous MYOD1/myogenin	Diffuse MYOD1/Myogenin	MYOD1 >myogenin	Scant MYOD1/myogenin
Genetic features	Drivers unknown	FOX01 fusion	VGLL2/NCOA2 fusions, TFCP2 fusions, MYOD1 activatingmutations	Complexgenetics

RMS, rhabdomyosarcomas.

Figure 6. Diffuse metastatic spread in a 60-year-old female with spindle cell/sclerosing RMS of the right thigh (arrow). Post-contrast CT depicts in a) coronal and b) sagittal reconstructions lung metastases (arrow), right hilar adenopathy (arrowhead), hepatic metastases (black arrows), pancreatic metastases (white asterisk), right renal metastases (black asterisks), and tumour deposits in the anterior abdominal wall (black arrowhead). RMS, rhabdomyosarcomas.

associated with an increase in ADC values) and may complement the assessment of tumour response after therapy, along with the early detection of local relapse after surgery.[12,13] Dynamic contrast-enhanced MRI (DCE-MRI) provides complementary information to detect necrosis by displaying low wash-in/out and time-to-peak rates.[13] Despite the imaging appearance of primary RMS being heterogeneous and non-specific, Allen et al outlined a radiologic-pathology correlation in a small cohort of patients.[14] aRMS, spindle-cell/sclerosing and pleomorphic subtypes tend to be highly heterogeneous due to vast necro-haemorrhagic components, whilst eRMS tends to be homogeneous with minimal central necrosis.[15]

In the local staging of the disease, MRI provides in-depth characterisation of the tumour relationship with surrounding organs and neurovascular bundles, which may hinder surgical resectability (Figure 12). The visualisation of peripheral nerves may possibly be complemented by echoplanar DWI with background

Figure 7. Same 22-year-old male patient in Figure 2c–d diagnosed with aRMS. (a) Ultrasound shows an 18G- core needle during percutaneous biopsy (arrow) of the hypoechoic mass in the hypothenar eminence. (b) Axial STIR image depicts a hyperintense, heterogeneous capsuled bulky mass. (c) ^{18}F-FDG-avid axillary lymphadenopathy (c) before and (d) after neoadjuvant chemotherapy. Similarly, the primary tumour was (e) ^{18}F-FDG-avid and showed f) a dramatic decrease in radiopharmaceutical uptake after induction therapy (arrow). ^{18}F-FDG, ^{18}F-fludeoxyglucose; STIR, short-tau inversion recovery.

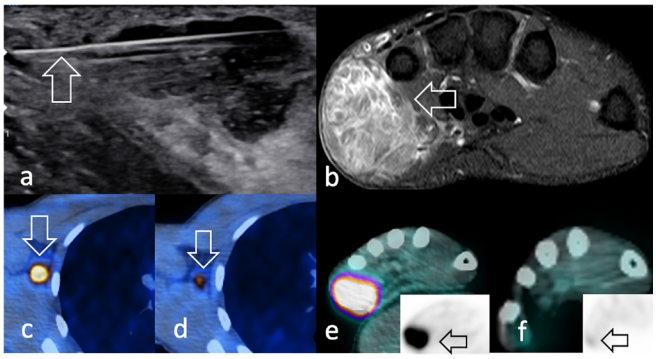

body signal suppression using a single b-value (around 700 s/mm^2), a technique named DW neurography (Figure 12c–d).[16] Dedicated post-processing softwares have been recently implemented to improve the conspicuity of the nerve roots on coronal maximum intensity projection (MIP) images, which are of great utility in displaying long nerve trajectories. Moreover, quantitative diffusion tensor imaging (DTI) neurography is emerging as a complementary tool to evaluate the microarchitecture of the nerve fibers through parameters like mean diffusivity and fractional anisotropy.[17]

Unlike most soft tissue sarcomas, regional and distant lymphadenopathies are typically encountered in RMS. They are often first detected at ultrasound and then confirmed at CT or MR, showing enlarged volume, eccentric cortical thickening and internal vascularised nodules or septa (Figure 13).

Distant metastases at diagnosis occur in more than 20% and are mostly located in the lungs.[7,8] CT or PET/CT are therefore the modalities of choice for distant staging (Figure 14). In this respect, a maximum diameter exceeding 5 mm is usually

Figure 8. A conglomerate retroperitoneal lymphadenopathy (arrow) is shown both (a) on ultrasound (arrow) and b) on axial contrast-enhanced CT (arrow) in a 18-year-old patient with eRMS of the tunica vaginalis. RMS, rhabdomyosarcomas.

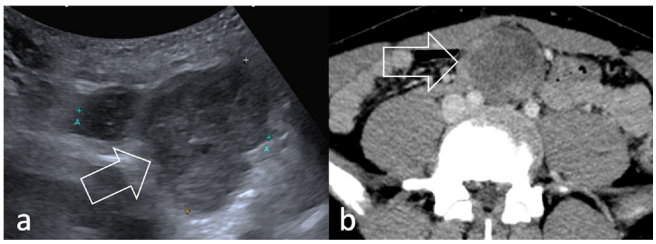

Figure 9. 15-year-old male with a pleomorphic RMS arising in the thyroid showing (a) heterogeneous echogenicity on ultrasound (arrow) and (b) on contrast enhancement at CT (arrows). RMS, rhabdomyosarcomas.

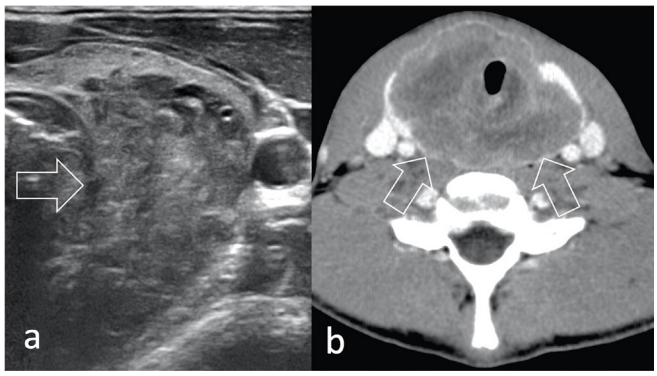

considered the cut-off value to consider a pulmonary nodule as a likely metastasis in high-grade sarcomas.[18] CT also provides high accuracy in assessing lytic cortical bone lesions and therefore complements the intramedullary bone assessment at MRI. Brain metastases are relatively rare and head contrast-enhanced MRI is required only in patients with neurologic symptoms.

PET and the added value of hybrid imaging

High-grade soft tissue sarcomas are mostly characterised by high mitotic count sustained by intense glycolytic activity. Hence, they can be well-displayed at ^{18}F-FDG PET, appearing as a hypermetabolic area with high radiopharmaceutical uptake. Although clinical applications of hybrid imaging in soft tissue sarcoma are potentially numerous, PET-based imaging is not routinely used for staging soft tissue sarcoma.[19] In fact, CT and MRI usually meet the needs of an accurate local and distant staging. However, the typical nodal, bone and bone marrow involvement encountered in RMS makes PET-based imaging of particular importance in the comprehensive evaluation of this disease. Solid evidence suggests whole-body ^{18}F- FDG PET/CT to represent the preferred staging and re-staging modality for RMS,

Figure 10. 50-year-old male with spindle cell/sclerosing RMS located in the inter scalene triangle (arrow) visualised (a) at T_2W and (b) at contrast-enhanced CT, involving right supraclavicular nodes, I° rib and the apex of the lung. The hyperintense lesion within the mass (asterisk) was revealed to be a neurofibroma. T_2 W, T_2 weighted,

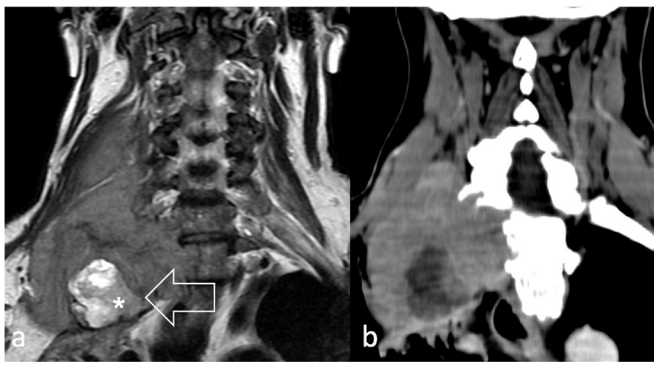

Figure 11. A 59-year-old male presenting with a lump in his left axilla. MRI showed on coronal T_2W (a) and T_1W after contrast-enhancement (b) a vascularised, extensively necrotic mass in the left axilla (arrow). Diagnosis of pleomorphic RMS was assigned after biopsy. After (c) partial response after chemotherapy (arrow), the lesion was surgically removed with radical intent and adjuvant radiation therapy was delivered. ^{18}F-FDG PET/CT performed 1 year later showed (d) minor uptake, consistent with chronic inflammation (arrow). ^{18}F-FDG, ^{18}F-fludeoxyglucose; PET, positron emision tomography; RMS, rhabdomyosarcomas; T_1W, T_1 weighted; T_2W, T_2 weighted.

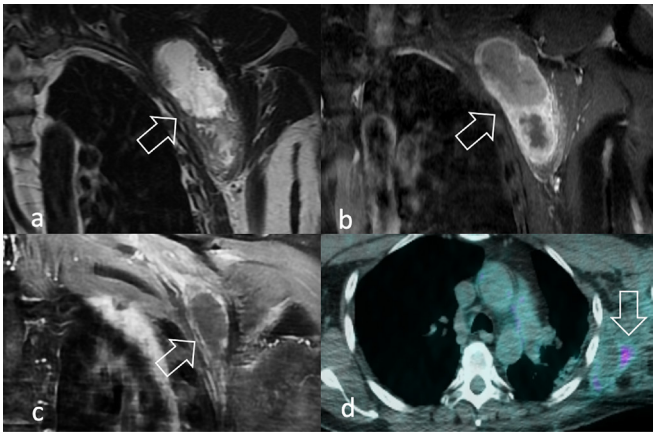

outperforming conventional imaging (CT, MRI, bone scintigraphy) in the assessment of local, regional and distant disease (86% *vs* 54% accuracy, respectively). A recent review confirmed this evidence, reporting PET/CT to change the management of RMS patients in 18% of cases.[20]

PET-based assessment is critically useful for the identification of regional or distant lymphatic spread. ^{18}F-FDG PET/CT detects lymph node involvement with 80–100% sensitivity and 89–100% specificity (Figure 15).[21] Nodal disease at diagnosis

Figure 13. 26-year-old male diagnosed with pleomorphic head and neck RMS. (a) ^{11}C-Methionine PET/CT shows the primary tumour as a round area of intense radiopharmaceutical uptake in the temporal fossa (arrow). (b) Color flow Doppler ultrasound of the neck shows a right lateral cervical lymph node with abnormal morphology, echogenicity and vascularization consistent with regional nodal involvement (arrow). RMS, rhabdomyosarcomas.

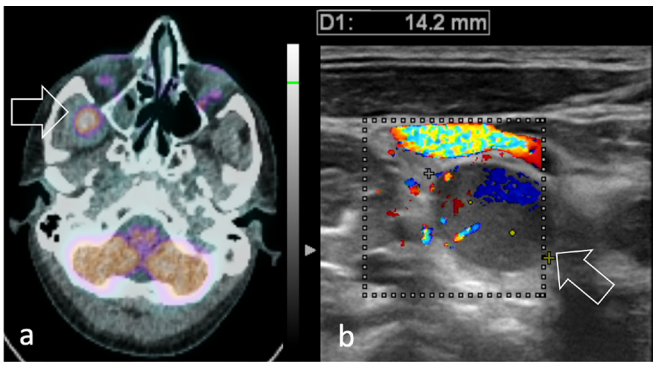

Figure 12. Same patient in Figure 2e–f. A 52-year-old male with pain in his right upper extremity during exercise. (a) T_1W image MRI shows an 8 cm diameter mass lying on the scaleni muscles, without (b) arterial involvement (c) DWI neurography displays the involvement of the brachial plexus compared to (d) the contralateral plexus. (e) Peripheral signal restriction (arrow) (f) mild radiopharmaceutical uptake (arrow) were identified at DWI and ^{18}F-FDG PET/CT, respectively. Biopsy revealed spindle cell/sclerosing RMS. ^{18}F-FDG, ^{18}F-fludeoxyglucose; DWI, diffusion-weighted imaging; PET, positron emision tomography; RMS, rhabdomyosarcomas; T_1W, T_1 weighted.

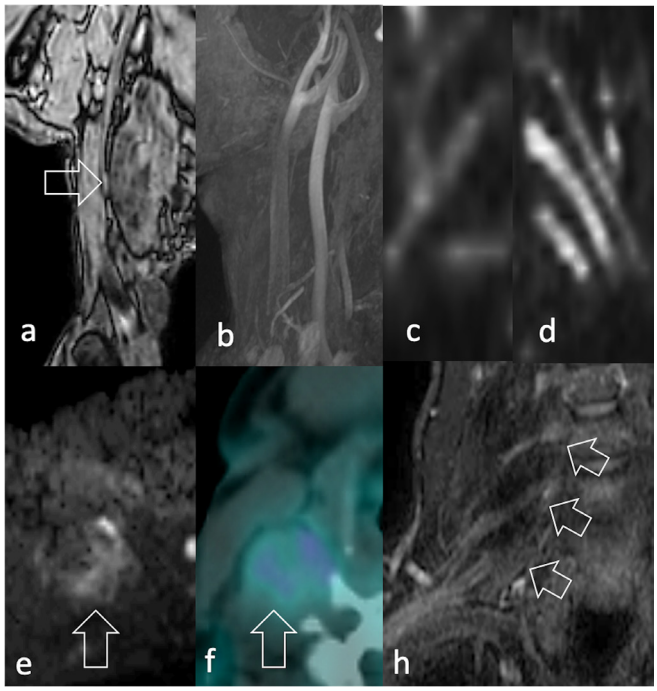

represents biological aggressiveness and is either the strongest predictive factor for failure of local tumour control and an independent negative prognostic factor of shorter 5-year overall survival.[21,22]

PET outperformed bone scintigraphy imaging in the assessment of bone involvement, which reduces 3-year event-free survival from 34 to 14%.[20] Possible explanations are that ^{18}F-FDG-PET/

Figure 14. ^{18}F-FDG PET/CT shows lung metastases (arrows) from a) pleomorphic heart RMS visualised in a 52-year-old woman after recent sternotomy (asterisk) and b) pleomorphic pulmonary RMS along with right paracardiac adenopathy in a 50-year-old man. FDG-avid primary pleomorphic pleural RMS is shown in a 80-year-old woman (arrow). ^{18}F-FDG, ^{18}F-fludeoxyglucose; PET, positron emision tomography; RMS, rhabdomyosarcomas.

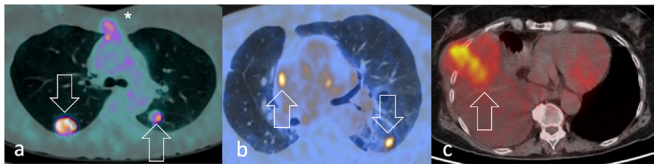

Figure 15. Coronal post-contrast CT scan detects (a) multiple, confluent axillary lymphadenopathies and (c) right diaphragmatic adenopathy (arrow) in a patient with aRMS. ^{18}F-FDG PET identifies (b) a tiny precrural and (d) retroperitoneal lymph node metastasis (arrow) in a 17-year-old patient diagnosed with nasal eRMS. ^{18}F-FDG, ^{18}F-fludeoxyglucose; PET, positron emision tomography; RMS, rhabdomyosarcomas.

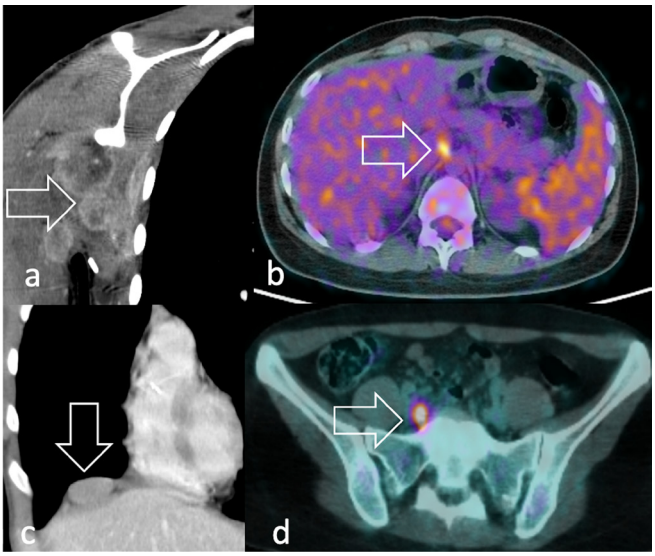

CT and bone scintigraphy rely on different mechanisms to detect tumour involvement. Whereas the first directly visualises the glucose uptake within the tumour, scintigraphy indirectly images the neoplastic involvement by displaying tumour-induced bone repair and remodelling. Such intrinsic differences may also significantly underestimate or overestimate the tumour response, considering that changes in bone structure in response to therapy can take several months to occur.[23] The high diagnostic accuracy of PET imaging may also possibly overcome the need for a bone marrow biopsy, which is still currently used for the definition of staging and prognosis (Figure 16).

Figure 16. Bone involvement in RMS can be either (a) sclerotic, permeative and poorly FDG-avid or (b) lytic and markedly FDG-avid at ^{18}F-FDG PET (arrow). In lytic lesions, (c) percutaneous cementoplasty (arrow) can be performed to achieve pain relief, like in the case of this 52-year-old female with pleomorphic RMS and osteoporosis. ^{18}F-FDG, ^{18}F-fludeoxyglucose; PET, positron emision tomography; RMS, rhabdomyosarcomas.

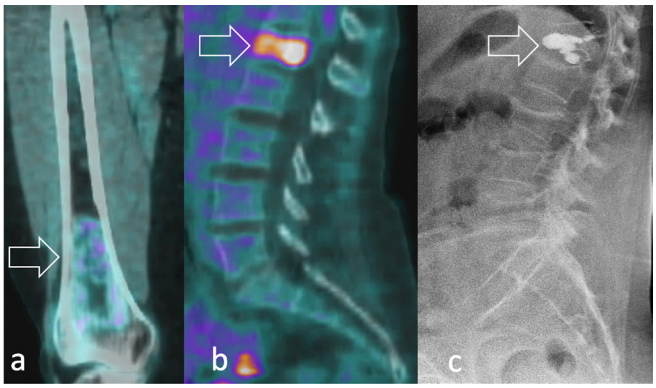

Figure 17. Same patient in Figure 2g–h. (a) Metastasis from pulmonary pleomorphic RMS in the left ventricle displayed at ^{18}F-FDG PET/T_2W-MRI (arrow). ^{18}F-FDG PET/CT images (b) retroperitoneal adenopathy (arrow) and (c) a distant FDG-avid metastasis in the anterior abdominal wall (arrow). ^{18}F-FDG, ^{18}F-fludeoxyglucose; PET, positron emision tomography; RMS, rhabdomyosarcomas; T_2W, T_2 weighted.

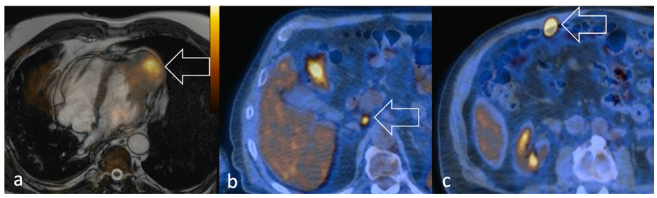

When imaging tumours in the head and neck area, the high physiological uptake of ^{18}F-FDG within the brain represents an important limitation particularly in the evaluation of intracranial infiltration. In an effort to overcome such drawbacks, other radiopharmaceuticals like ^{11}C-methionine (Figures 4 and 13) and ^{11}C-choline have been introduced for the imaging of skull base, head, neck and brain tumours.[24] Similarly to ^{18}F-FDG PET, ^{11}C-choline PET/CT was shown to be superior to CT, MRI and scintigraphy in the assessment of local, regional and distant disease stage (94% *vs* 50% accuracy, respectively), especially lymph node and bone disease. Moreover, it increased specificity in detecting lung metastases.[25] Detection of lymph node involvement is further refined when ^{11}C-choline PET/CT is used instead of conventional imaging (100% *vs* 63% accuracy, respectively). In the detection of recurrent tumours, PET/CT may play a complementary role to MRI in discriminating local tumour recurrence from post-therapeutic tissue changes, especially when peritumoral oedema is present.[26] Unlike PET/CT, PET/MRI is still a rarity in the clinical scenario. This notwithstanding, it is possible to combine PET and MRI acquired separately at different times, although motion artefacts and partial volume effects may alter the quality of the final imaging.[27]

Radiotherapy takes considerable benefit from PET/MRI, since the combination of the two provides better delineation of ill-defined tumours for treatment planning.[28] Moreover, the exquisite anatomic details and the functional insights of tumour biology provided by both PET and MRI may improve the assessment of soft tissue distant metastases (Figure 17).

Despite its clinical use still being limited, PET/MRI has the potential to provide further improvement in the functional evaluation of tumour changes after therapy and represent a substantial benefit in the management of RMS in adolescent and adult patients, given that the estimated cumulative radiation dose is nearly five times lower than PET/CT.[29] The main limitations of PET-based hybrid imaging are false-positive reactive lymph nodes – a common finding in regional lymph nodes after percutaneous biopsy, and true-positive metastatic lymph nodes located close to sites of physiologic high radiotracer accumulation (urinary bladder, brain, and heart in case of ^{18}F-FDG).[30]

Treatment of adult RMS

Given its rarity and complexity, the management of adult RMS should be centralised in selected centres with a multidisciplinary expertise in sarcoma.[31]

The introduction of intense, multidrug regimens has contributed to substantial improvements in the prognosis of RMS patients. In fact, like other small round cell tumours, aRMS and eRMS are chemosensitive tumours with more than 85% dimensional response according to RECIST 1.1.[7] Chemotherapy thus represents a first-line approach even in the case of localised RMS, also considering the high risk of systemic spread at initial diagnosis. Unlike paediatric patients, which are treated with different chemotherapy regimens according to specific risk categories,[32] aRMS and eRMS are always treated with high-dose multidrug combinations including vincristine, doxorubicin, ifosfamide, and etoposide. Local treatment varies according to tumour location and response to chemotherapy. When feasible, surgery aims to achieve radical excision through a wide resection with adequate tumour margins. Radiation therapy can be delivered both in a pre-/post-operative setting, but pre-operative RT (alone or combined with chemotherapy) is preferred since the treatment field size is smaller, reduces tumour cellularity, and allows downstaging of disease. However, considering the high radiosensitivity of RMS, it may also represent the exclusive treatment modality for local control when demolitive surgery is not an option. Regional lymphadenectomy or irradiation should always be performed in case of positive nodes.[33]

The management of the pleomorphic RMS diverges considerably from aRMS and eRMS variants due to its poor chemo/radiosensitivity. Surgery followed by radiation therapy represents the standard treatment, but pre-operative doxorubicin-based chemotherapy may possibly be considered when surgery is not feasible. Finally, the spindle cell/sclerosing variant is generally treated with surgery and/or exclusive radiation therapy given the limited chemosensitivity.

Radiation therapy and/or percutaneous treatments, like cementoplasty or ablation, represent an effective option to treat oligometastatic patients or achieve rapid pain relief in symptomatic patients (Figure 16).[34,35]

FUTURE TRENDS IN IMAGING

The recent trends in imaging research of RMS include assessing the role of functional imaging (DCE-MRI, DWI and PET) in the prediction of tumour response after neoadjuvant therapies and in the early identification of tumour recurrence.[20] Unravelling the predictive value of ADC and SUV is an intriguing task, especially when areas of photopenic ^{18}F-FDG uptake coincide on areas characterised by low ADC values.[36] Absolute parameters extracted from DWI and intravoxel incoherent motion (IVIM) have recently been correlated with Ki67 proliferation index in murine models of RMS, representing a further step in the awareness of biological information enclosed in diffusion based-imaging.[37] In a preclinical setting, PET tracers like ^{18}F-FAZA PET and ^{18}F-FMISO are promising labelled-molecules reflecting tumour hypoxia, which would encourage radiotherapy escalation through hypoxic radiosensitisers or identification of areas requiring radiotherapy boost.[38] Being conventional imaging still far from providing an accurate histological characterisation in sarcoma patients, advanced image analysis is showing promising results in the differential diagnosis of RMS and may complement the information coming from conventional imaging and histology. In this regard, a deep-learning-based computer-aided diagnosis (CADx)system was able to discriminate embryonal from alveolar RMS solely by analysing multi parametric MR images.[39] Recent early clinical experiences using ^{68}Ga-Ga-DOTA-FAPI-04 PET/CT have reported a better sensitivity and accuracy for the detection of both primary and metastatic lesions than did ^{18}F-FDG PET/CT. As ^{68}Ga- Ga-DOTA-FAPI-04 PET/CT strongly accumulates in those cancers characterised by a prominent desmoplastic reaction, soft tissue sarcoma resulted among the tumours with the highest uptake. With regard to RMS, this new radiotracer seems particularly promising as it was shown to be superior to ^{18}F-FDG PET/CT both in the nodal staging and in the detection of bone metastasis.[40,41]

CONCLUSIONS

An effective collaboration between clinicians and radiologists in referral sarcoma centres bears the potential to guide the clinical management of adult RMS. Besides morphological assessment through conventional cross-sectional imaging, hybrid imaging combining PET with CT or MRI has been established as a reliable tool to better define the extent of adult RMS, especially with regard to lymph node and bone marrow involvement. In light of recent developments in hybrid imaging, the radiological characterisation of tumour response after treatment and its correlation with clinical outcome represents an ambitious goal to personalise multimodal treatment in an extremely rare cancer like adult RMS.

REFERENCES

1. WHO Classification of Tumours of Soft Tissue and Bone.. Available from: http://apps.who.int/bookorders/anglais/detart1.jsp?codlan=1&codcol=70&codcch=4005 [cited 2020May28].
2. van der Graaf WTA, Orbach D, Judson IR, Ferrari A. Soft tissue sarcomas in adolescents and young adults: a comparison with their paediatric and adult counterparts. *Lancet Oncol* 2017; **18**: e166–75. doi: https://doi.org/10.1016/S1470-2045(17)30099-2
3. Renne SL. Who, how and what of pathology of soft tissue sarcoma. *Chin Clin Oncol* 2018;: 100909 Nov 2018. doi: https://doi.org/10.21037/cco.2018.10.09
4. Trojani M, Contesso G, Coindre JM, Rouesse J, Bui NB, de Mascarel A, et al. Soft-Tissue sarcomas of adults; study of pathological prognostic variables and definition of a histopathological grading system. *Int J*

Cancer 1984; **33**: 37–42. doi: https://doi.org/10.1002/ijc.2910330108
5. Coindre J-M. Grading of soft tissue sarcomas: review and update. *Arch Pathol Lab Med* 2006; **130**: 1448–53. doi: https://doi.org/10.1043/1543-2165(2006)130[1448:GOSTSR]2.0.CO;2
6. Leiner J, Le Loarer F. The current landscape of rhabdomyosarcomas: an update. *Virchows Arch* 2020; **476**: 97-108. doi: https://doi.org/10.1007/s00428-019-02676-9
7. Ferrari A, Dileo P, Casanova M, Bertulli R, Meazza C, Gandola L, et al. Rhabdomyosarcoma in adults. A retrospective analysis of 171 patients treated at a single institution. *Cancer* 2003; **98**: 571–80. doi: https://doi.org/10.1002/cncr.11550
8. Bisogno G, Compostella A, Ferrari A, Pastore G, Cecchetto G, Garaventa A, et al. Rhabdomyosarcoma in adolescents: a report from the AIEOP soft tissue sarcoma Committee. *Cancer* 2012; **118**: 821–7. doi: https://doi.org/10.1002/cncr.26355
9. Romualdi C, De Pittà C, Tombolan L, Bortoluzzi S, Sartori F, Rosolen A, et al. Defining the gene expression signature of rhabdomyosarcoma by meta-analysis. *BMC Genomics* 2006; **7**: 287. doi: https://doi.org/10.1186/1471-2164-7-287
10. Sultan I, Qaddoumi I, Yaser S, Rodriguez-Galindo C, Ferrari A. Comparing adult and pediatric rhabdomyosarcoma in the surveillance, epidemiology and end results program, 1973 to 2005: an analysis of 2,600 patients. *J Clin Oncol* 2009; **27**: 3391–7. doi: https://doi.org/10.1200/JCO.2008.19.7483
11. Komdeur R, Klunder J, van der Graaf WTA, van den Berg E, de Bont ESJM, Hoekstra HJ, et al. Multidrug resistance proteins in rhabdomyosarcomas: comparison between children and adults. *Cancer* 2003; **97**: 1999–2005. doi: https://doi.org/10.1002/cncr.11259
12. Del Grande F, Subhawong T, Weber K, Aro M, Mugera C, Fayad LM. Detection of soft-tissue sarcoma recurrence: added value of functional MR imaging techniques at 3.0 T. *Radiology* 2014; **271**: 499–511. doi: https://doi.org/10.1148/radiol.13130844
13. Soldatos T, Ahlawat S, Montgomery E, Chalian M, Jacobs MA, Fayad LM. Multiparametric assessment of treatment response in high-grade soft-tissue sarcomas with anatomic and functional MR imaging sequences. *Radiology* 2016; **278**: 831–40. doi: https://doi.org/10.1148/radiol.2015142463
14. Allen SD, Moskovic EC, Fisher C, Thomas JM. Adult rhabdomyosarcoma: cross-sectional imaging findings including histopathologic correlation. *AJR Am J Roentgenol* 2007; **189**: 371–7. doi: https://doi.org/10.2214/AJR.07.2065
15. Saboo SS, Krajewski KM, Zukotynski K, Howard S, Jagannathan JP, Hornick JL, et al. Imaging features of primary and secondary adult rhabdomyosarcoma. *AJR Am J Roentgenol* 2012; **199**: W694–703. doi: https://doi.org/10.2214/AJR.11.8213
16. Andreou A, Sohaib A, Collins DJ, Takahara T, Kwee TC, Leach MO, et al. Diffusion-Weighted Mr neurography for the assessment of brachial plexopathy in oncological practice. *Cancer Imaging* 2015; **15**: 6. doi: https://doi.org/10.1186/s40644-015-0041-5
17. Mazal AT, Faramarzalian A, Samet JD, Gill K, Cheng J, Chhabra A. Mr neurography of the brachial plexus in adult and pediatric age groups: evolution, recent advances, and future directions. *Expert Rev Med Devices* 2020; **17**: 111–22. doi: https://doi.org/10.1080/17434440.2020.1719830
18. Nakamura T, Matsumine A, Matsusaka M, Mizumoto K, Mori M, Yoshizaki T, et al. Analysis of pulmonary nodules in patients with high-grade soft tissue sarcomas. *PLoS One* 2017; **12**: e0172148. doi: https://doi.org/10.1371/journal.pone.0172148
19. Nanni C, Fanti S. Fdg-Pet and PET/CT for evaluating soft tissue sarcomas. *PET Clin* 2010; **5**: 341–7. doi: https://doi.org/10.1016/j.cpet.2010.04.005
20. Lim HJ, Johnny Ong C-A, Tan JW-S, Ching Teo MC. Utility of positron emission tomography/computed tomography (PET/CT) imaging in the evaluation of sarcomas: a systematic review. *Crit Rev Oncol Hematol* 2019; **143**: 1–13. doi: https://doi.org/10.1016/j.critrevonc.2019.07.002
21. Rosenthal J, Cardona K, Sayyid SK, Perricone AJ, Reimer N, Monson D, et al. Nodal metastases of soft tissue sarcomas: risk factors, imaging findings, and implications. *Skeletal Radiol* 2020; **49**: 221-229. doi: https://doi.org/10.1007/s00256-019-03299-6
22. Khosla D, Sapkota S, Kapoor R, Kumar R, Sharma SC. Adult rhabdomyosarcoma: clinical presentation, treatment, and outcome. *J Cancer Res Ther* 2015; **11**: 830–4. doi: https://doi.org/10.4103/0973-1482.144637
23. Guimarães JB, Rigo L, Lewin F, Emerick A. The importance of PET/CT in the evaluation of patients with Ewing tumors. *Radiol Bras* 2015; **48**: 175–80. doi: https://doi.org/10.1590/0100-3984.2013.1887
24. Ito K, Matsuda H, Kubota K, Spectrum I. Imaging Spectrum and Pitfalls of (11)C-Methionine Positron Emission Tomography in a Series of Patients with Intracranial Lesions. *Korean J Radiol* 2016; **17**: 424–34. doi: https://doi.org/10.3348/kjr.2016.17.3.424
25. Shaban EAIN. The usefulness of 18-F-FDG PET/CT for detection of adult soft tissue sarcomas local recurrence and distant metastases. *The Egyptian Journal of Radiology and Nuclear Medicine* 2018; **49**: 1052–9. doi: https://doi.org/10.1016/j.ejrnm.2018.05.014
26. Erfanian Y, Grueneisen J, Kirchner J, Wetter A, Podleska LE, Bauer S, et al. Integrated 18F-FDG PET/MRI compared to MRI alone for identification of local recurrences of soft tissue sarcomas: a comparison trial. *Eur J Nucl Med Mol Imaging* 2017; **44**: 1823–31. doi: https://doi.org/10.1007/s00259-017-3736-y
27. Parikh N, Friedman KP, Shah SN, Chandarana H. Practical guide for implementing hybrid PET/MR clinical service: lessons learned from our experience. *Abdom Imaging* 2015; **40**: 1366–73. doi: https://doi.org/10.1007/s00261-015-0444-6
28. Zhu T, Das S, Wong TZ. Integration of PET/MR hybrid imaging into radiation therapy treatment. *Magn Reson Imaging Clin N Am* 2017; **25**: 377–430. doi: https://doi.org/10.1016/j.mric.2017.01.001
29. Partovi S, Kohan AA, Zipp L, Faulhaber P, Kosmas C, Ros PR, et al. Hybrid PET/MR imaging in two sarcoma patients - clinical benefits and implications for future trials. *Int J Clin Exp Med* 2014; **7**: 640–8.
30. Gabriel M, Rubello D. 18F-Fdg PET-CT in soft tissue sarcomas: staging, restaging, and prognostic value? *Nucl Med Commun* 2016; **37**: 3–8. doi: https://doi.org/10.1097/MNM.0000000000000407
31. Blay J-Y, Soibinet P, Penel N, Bompas E, Duffaud F, Stoeckle E, et al. Improved survival using specialized multidisciplinary board in sarcoma patients. *Ann Oncol* 2017; **28**: 2852–9. doi: https://doi.org/10.1093/annonc/mdx484
32. Raney RB, Maurer HM, Anderson JR, Andrassy RJ, Donaldson SS, Qualman SJ, et al. The intergroup rhabdomyosarcoma Study Group (IRSG): major lessons from the IRS-I through IRS-IV studies as background for the current IRS-V treatment protocols. *Sarcoma* 2001; **5**: 9–15. doi: https://doi.org/10.1080/13577140120048890
33. Bergamaschi L, Bertulli R, Casanova M, Provenzano S, Chiaravalli S, Gasparini P, et al. Rhabdomyosarcoma in adults: analysis of treatment modalities in a prospective single-center series. *Med Oncol* 2019; **36**: 59. doi: https://doi.org/10.1007/s12032-019-1282-0
34. Gennaro N, Sconfienza LM, Ambrogi F, Boveri S, Lanza E. Thermal ablation to relieve pain from metastatic bone disease: a

systematic review. *Skeletal Radiol* 2019; **48**: 1161–9. doi: https://doi.org/10.1007/s00256-018-3140-0

35. Gronchi A, Guadagnolo BA, Erinjeri JP. Local ablative therapies to metastatic soft tissue sarcoma. *Am Soc Clin Oncol Educ Book* 2016; **35**: e566–75. doi: https://doi.org/10.1200/EDBK_157450
36. Pourmehdi Lahiji A, Jackson T, Nejadnik H, von Eyben R, Rubin D, Spunt SL, et al. Association of Tumor [^{18}F]FDG Activity and Diffusion Restriction with Clinical Outcomes of Rhabdomyosarcomas. *Mol Imaging Biol* 2019; **21**: 591–8. doi: https://doi.org/10.1007/s11307-018-1272-1
37. Yuan Y, Zeng D, Liu Y, Tao J, Zhang Y, Yang J, et al. Dwi and IVIM are predictors of Ki67 proliferation index: direct comparison of MRI images and pathological slices in a murine model of rhabdomyosarcoma. *Eur Radiol* 2019;.
38. Sigal IR, Sebro R. Preclinical PET tracers for the evaluation of sarcomas: understanding tumor biology. *Am J Nucl Med Mol Imaging* 2018; **8**: 428–40.
39. Banerjee I, Crawley A, Bhethanabotla M, Daldrup-Link HE, Rubin DL. Transfer learning on fused multiparametric Mr images for classifying histopathological subtypes of rhabdomyosarcoma. *Comput Med Imaging Graph* 2018; **65**: 167–75. doi: https://doi.org/10.1016/j.compmedimag.2017.05.002
40. Kratochwil C, Flechsig P, Lindner T, Abderrahim L, Altmann A, Mier W, et al. ^{68}Ga-FAPI PET/CT: Tracer Uptake in 28 Different Kinds of Cancer. *J Nucl Med* 2019; **60**: 801–5. doi: https://doi.org/10.2967/jnumed.119.227967
41. Chen H, Pang Y, Wu J, Zhao L, Hao B, Wu J, et al. Comparison of [68Ga]Ga-DOTA-FAPI-04 and [18F] FDG PET/CT for the diagnosis of primary and metastatic lesions in patients with various types of cancer. *Eur J Nucl Med Mol Imaging* 2020;.